

# High Step-UP DC-DC Converter Using Cascode Technique

J.Shankaraiah, G.Kumara Swamy and Dr.K.Sri Gowri

**Abstract** — A transformer less high step-up DC-DC converter is investigated in this paper. Two buck-boost converters are integrated with single switch. The input voltage of the front semi-stage is the DC source. The input voltage of the rear semi-stage is the series of the DC source and the output voltage of the front semi-stage. Moreover, the output voltage of the proposed converter is the output voltages of the two semi-stage by cascode. Thus, high step-up voltage gain can be achieved with appropriate duty ratio. The operating principle and steady-state analysis of the proposed converter are discussed in detailed. Finally, a laboratory prototype circuit is implemented to verify the performance.

**Keywords:** buck-boost converter, high step-up voltage gain, cascode technique.

## I. INTRODUCTION

High step-up DC-DC converters are used in many applications, such as renewable energy conversion, uninterruptible power supplies (UPS), and high intensity discharge (HID) lamp for automobile headlamp. Fig. 1 shows the fuel-cell electric conversion system. The high step-up DC-DC converter is required to boost the fuel-cell output voltage 24 - 40 V up to 200 V to supply power to the rear stage - inverter. In order to achieve high voltage gain, the conventional boost converter must be operated at extremely high duty ratio. However, due to the impacts of the parasitic resistive components and the reverse-recovery problem of the diodes, the conventional boost converter can not achieve high voltage gain. The DC-DC flyback converter is a very simple structure with high step-up voltage gain and electrical isolation. However, the active switch of these converters will suffer high voltage stress due to the leakage inductance of the transformer. For recycling the energy of the leakage inductance and minimizing the voltage stress on the active switch, some energy-regeneration techniques have proposed to clamp the voltage stress on the active switch and to recycle the leakage-inductance energy. This paper proposes a transformerless high step-up DCDC converter. The high step-up voltage can be achieved by using the cascode technique. The operating principle is described in section II. The steady-state analysis of the proposed converter is discussed in section III. The experimental results are presented in section IV. Finally, the conclusion is given in section V.

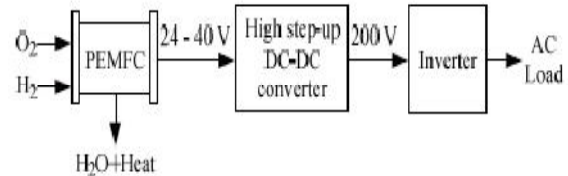


Fig. 1. Fuel-cell electric conversion system.

## II. OPERATING PRINCIPLES OF THE PROPOSED CONVERTER

Fig.2 shows the circuit configuration of the proposed converter, which includes one switch S, three diodes D1, Do1, and Do2, inductors L1 and L2, and output capacitors Co1 and Co2. Two buck-boost converters are integrated into the proposed converter by using single switch. The input voltage of the front semi-stage is the DC source and the input voltage of the rear semi-stage comes from the DC source and the output voltage of the front semi-stage by series. Moreover, the output voltage of the proposed converter comes from the output voltages of the two semi-stage by cascode. Thus, high step-up voltage gain can be achieved without extremely large duty ratio. Some typical waveforms are shown in Fig. 3. In order to simply the analysis of the operating principle, some conditions are assumed as follows:

- (i) Diodes D1, Do1, and Do2 are ideal.
- (ii) The capacitors Co1 and Co2 are enough large. Thus, the output voltage can be considered as constant.

When the proposed converter in continuous conduction mode (CCM), the operating principles are described as follows:

**Mode I:** During this time interval  $[t_0, t_1]$ , S is turned on. The equivalent circuit is shown in Fig. 4(a). The energy is transferred from the DC source to inductor L1 through switch S and diode D1. Also, the DC source and capacitor Co1 are series to release their energies to inductor L2 through switch S. So, the inductor currents  $i_{L1}$  and  $i_{L2}$  are increased linearly. Moreover, the energies stored in capacitors Co1 and Co2 are discharged to the load by series. At  $t = t_1$ , the mode is end when switch S is turned off. Thus, the voltages across inductors L1 and L2 are given as

$$V_{L1} = V_{in} \quad (1)$$

$$V_{L2} = V_{in} + V_{Co1} \quad (2)$$

J.Shankaraiah is a PG-Student, Dep. Of EEE, RGM CET, Nandyal, india. Email:sankar3ysrs@gmail.com, G.Kumara Swamy working as Assoc.Professor, Dept. Of EEE, RGM CET, Nandyal, india. Email:kumar1718@gmail.com and Dr.K.Sri Gowri, Professor, Dept. Of EEE, RGM CET, Nandyal, india. Email:gowrivasu.3@gmail.com

From equations (1) and (2), the inductor currents  $i_{L1}$  and  $i_{L2}$  are derived as follows:

$$i_{L1}(t) = i_{L1}(t_0) + \frac{V_{in}}{L_1}(t - t_0) \quad (3)$$

$$i_{L2}(t) = i_{L2}(t_0) + \frac{V_{in} + V_{Co1}}{L_2}(t - t_0) \quad (4)$$

**Mode II:** During this time interval  $[t1, t2]$ , switch S is turned off. The equivalent circuit is shown in Fig. 4(b). The energies stored in inductors L1 and L2 are released to the parasitic capacitor Cds. The energies stored in capacitors Co1 and Co2 are discharged to the load by series. At  $t = t2$ , the voltage across capacitor Cds is charged to  $V_{in} + V_{Co1}$  and this mode is end.

**Mode III:** During this time interval  $[t2, t3]$ , switch S is still turned off. Since the voltage across capacitor Cds is equal to  $V_{in} + V_{Co1}$  at  $t = t2$ . Then, diode Do1 is ON. The equivalent circuit is shown in Fig. 4(c). The energy stored in inductor L2 is still released to capacitor Cds. The energy stored in inductor L1 is released to capacitor Co1 and the load. Thus, the inductor current  $i_{L1}$  is decreased linearly. Also, the energy stored in capacitor Co2 is discharged to the load. At  $t = t3$ , the voltage across capacitor Cds is charged to  $V_{in} + V_o$  and the mode is end.

**Mode IV:** During this time interval  $[t3, t4]$ , switch S is still turned off. Since the voltage across capacitor Cds is equal to  $V_{in} + V_o$  at  $t = t3$ . Then, diodes Do1 and Do2 are ON. The equivalent circuit is shown in Fig. 4(d). The energies stored in inductors L1 and L2 are released to capacitors Co1, Co2, and the load. Thus, the inductor currents  $i_{L1}$  and  $i_{L2}$  are decreased linearly. At  $t = t4$ , switch S is turned on again and the mode is end. Thus, the voltages across inductors L1 and L2 are derived as follows:

$$V_{L1} = -V_{Co1} \quad (5)$$

$$V_{L2} = -V_{Co2} \quad (6)$$

From equations (3) and (4), the inductor currents  $i_{L1}$  and  $i_{L2}$  are obtained as

$$i_{L1}(t) = -\frac{V_{Co1}}{L_1}(t - t_3) + i_{L1}(t_3) \quad (7)$$

$$i_{L2}(t) = -\frac{V_{Co2}}{L_2}(t - t_3) + i_{L2}(t_3) \quad (8)$$

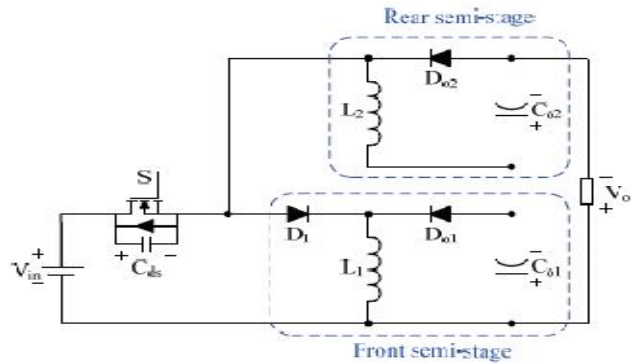


Fig. 2. Circuit configuration of the proposed converter.

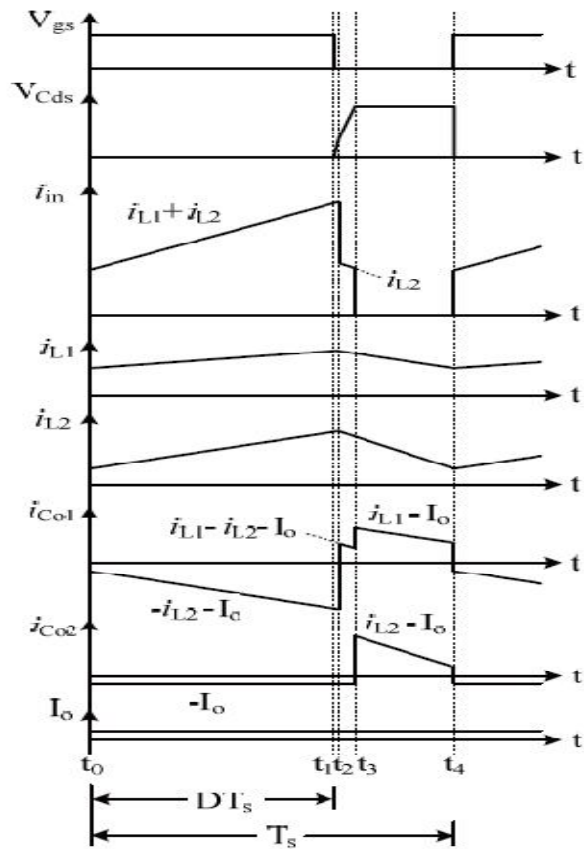
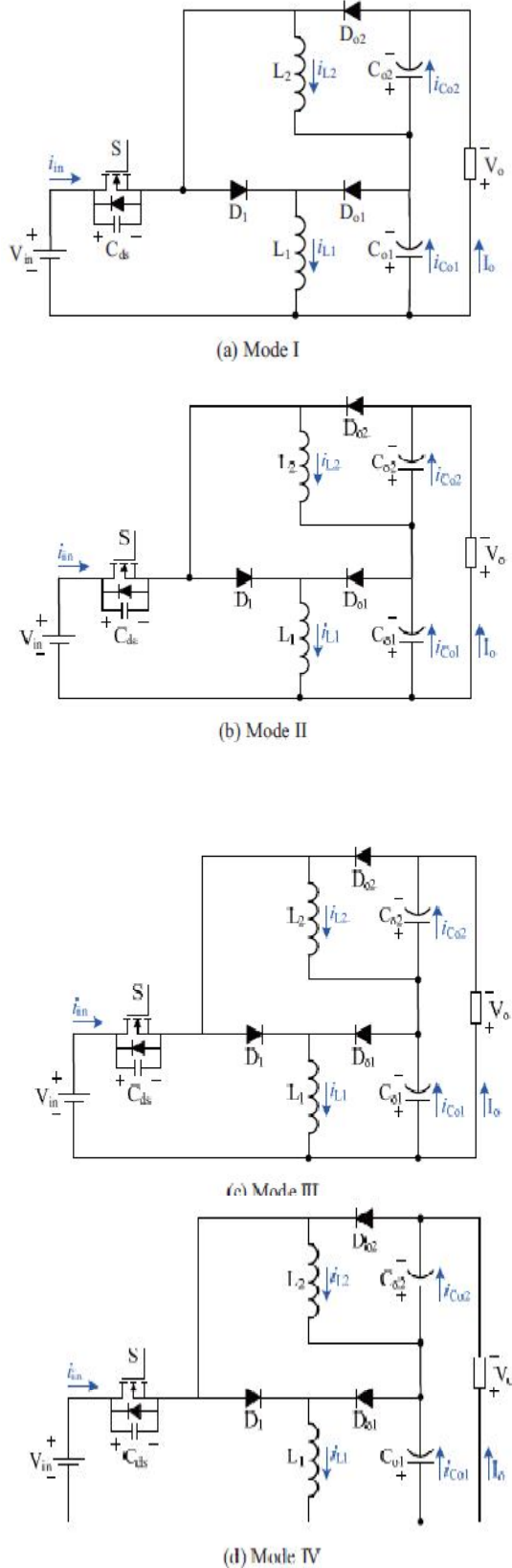


Fig. 3. Typical waveforms of the proposed converter in CCM operation.



**Fig. 4. Operating modes of the proposed converter.**

**III. STEADY STATE ANALYSIS**

In order to simplify the steady-state analysis, the time intervals of mode II and III are ignored since they are very short as compared to one switching cycle. Therefore, the time intervals of mode I and IV are considered as  $DT_s$  and  $(1-D)T_s$  respectively, where  $D$  is the duty ratio and  $T_s$  is the switching period. To apply the volt-second balance principle in inductors  $L_1$  and  $L_2$ . From equations (1), (2), (5), and (6), the following equations are given as:

$$V_{in}DT_s = V_{Co1}(1-D)T_s \tag{9}$$

$$(V_{in} + V_{Co1})DT_s = V_{Co2}(1-D)T_s \tag{10}$$

From equations (9) and (10), the following equations are derived as

$$\frac{V_{Co1}}{V_{in}} = \frac{D}{1-D} \tag{11}$$

$$\frac{V_{Co2}}{V_{in}} = \frac{D}{(1-D)^2} \tag{12}$$

Since  $V_o$  is equal to  $V_{Co1} + V_{Co2}$ . From equations (11) and (12), the voltage gain of the proposed converter is given by

$$M = \frac{V_o}{V_{in}} = \frac{2D - D^2}{(1-D)^2} \tag{13}$$

Thus, the curves of the voltage gain of the boost converter and the proposed converter are plotted in Fig. 5. It can be seen that the voltage gain of the proposed converter is larger than the voltage gain of the boost converter when the duty ratio is larger than 0.39. Thus, high step-up voltage gain can be achieved.

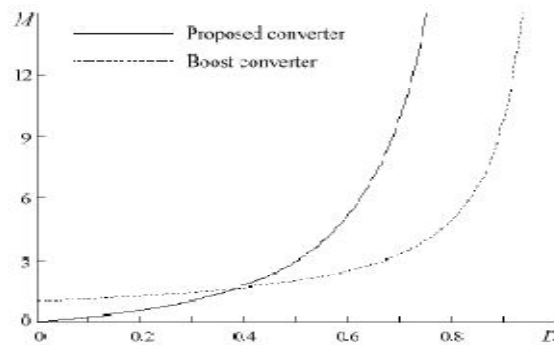


**Fig. 5. Voltage gains versus duty ratio for the proposed converter and the boost converter.**

**IV. SIMULATION RESULTS**

To verify the performance of the proposed converter, a prototype circuit is built in the laboratory, as shown in Fig. 6.

The circuit specifications and components are selected as input voltage  $V_{in} = 24\text{ V}$ , output voltage  $V_o = 200\text{ V}$ , output power  $P_o = 100\text{ W}$ , switching frequency  $f_s = 50\text{ kHz}$ , capacitors  $C_{o1} = C_{o2} = 680\text{ F}$ , inductors  $L_1 = 53\text{ H}$ , and  $L_2 = 636\text{ H}$ . Some experimental results are shown in Fig. 7 --- 10. Figs. 7 and 8 show some waveforms under the light-load condition  $P_o = 20\text{ W}$ . It is seen from Fig. 7 that the inductor currents  $i_{L1}$  and  $i_{L2}$  are discontinuous, which means that the upper cell and the lower cell of the proposed converter are operated in discontinuous conduction mode at the light-load condition. Moreover, the output voltage is well controlled at  $200\text{ V}$ . Fig. 8 shows the waveforms of  $V_{gs}$ ,  $i_{in}$ ,  $i_{Do1}$ , and  $i_{Do2}$ . Figs. 9 and 10 show some waveforms under the full-load condition  $P_o = 100\text{ W}$ . From Fig. 9, one can see that the inductor currents  $i_{L1}$  and  $i_{L2}$  are continuous, which means that the upper cell and the lower cell of the proposed converter are operated in continuous conduction mode at the full-load condition. Moreover, the output voltage is well controlled at  $200\text{ V}$ . Fig. 10 shows the waveforms of  $V_{gs}$ ,  $i_{in}$ ,  $i_{Do1}$ , and  $i_{Do2}$ . The measured results under various load conditions are described in table I and the curve of the measured efficiency is shown in Fig. 11. The conversion efficiency is  $72.7\%$  at the full-load condition.

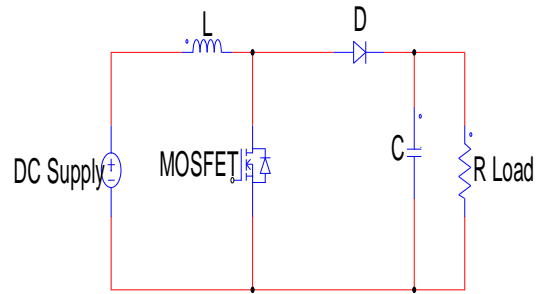


**Fig 7. Basic Circuit of Boost Converter**

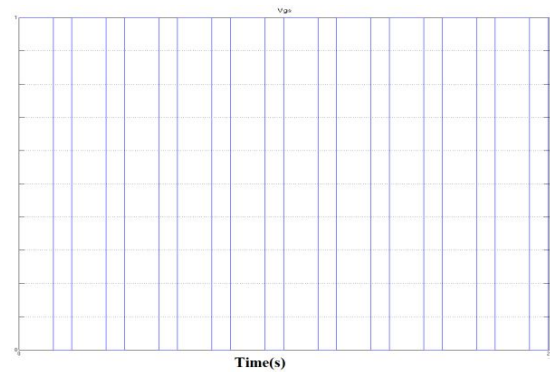


**Fig 8. Gate Pulse of Vgs**

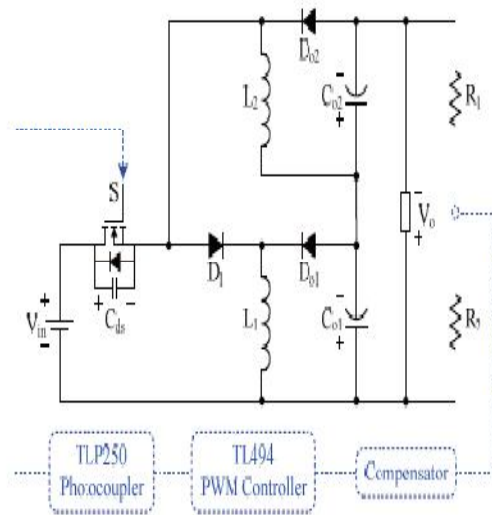


**Fig. 6. Prototype circuit of the proposed cascode converter.**

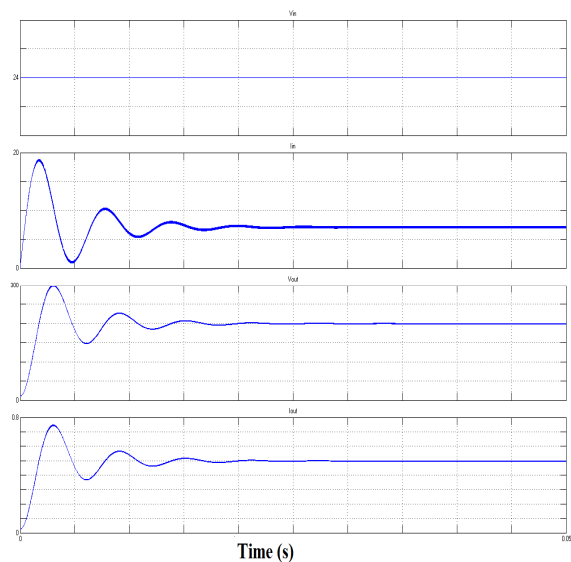


**Fig 9. Output Waveforms of Boost Converter**

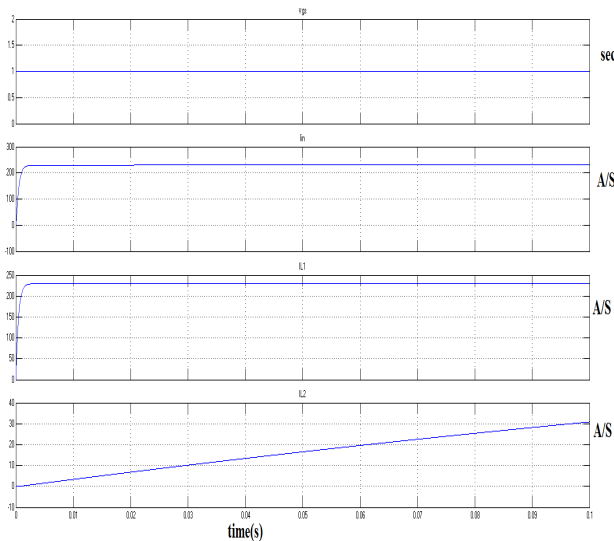


Fig 10. Waveforms of Closed loop Cascode Inductor Currents

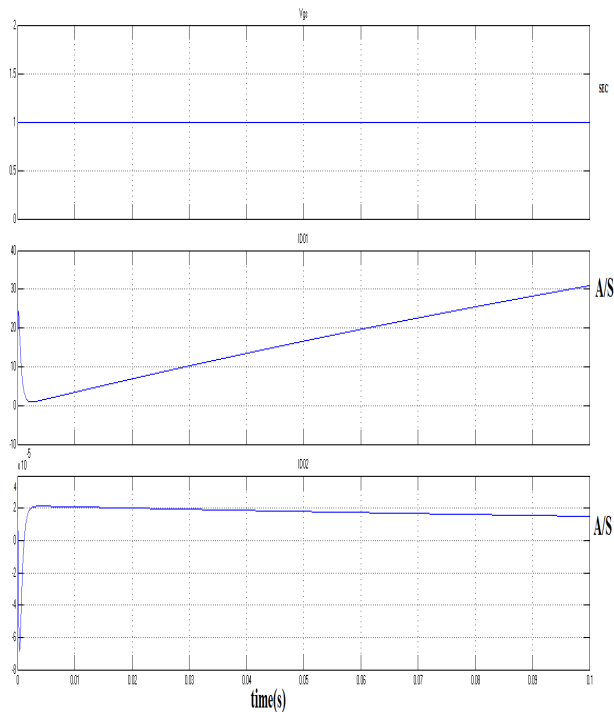


Fig 11. Waveforms of Closed loop Cascode Diode Currents

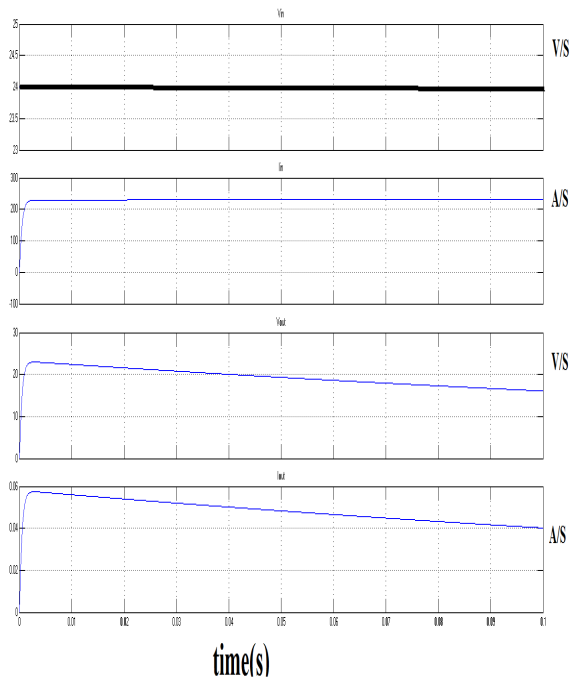


Fig 12. Waveforms of Vs, Lin, Vout & ILoad Of Closed Loop Cascode

V. CONCLUSIONS

The drawbacks in linear regulators are overcome by Switched-mode Regulators. Switch-mode DC to DC converters convert one DC voltage level to another, by storing the input energy temporarily and then releasing that energy to the output at a different voltage. This conversion method is more power efficient than linear voltage regulation. The basic converter topologies of switched-mode converters are Buck, Boost and Buck-Boost. This can be achieved by cascading of buck-boost converters with acceptable duty ratio.

A high step-up DC-DC cascaded buck-boost converter is presented. The operation and design aspects of the converter are discussed. The simulation of the converter circuit is carried out in MATLAB/SIMULINK. Simulation results are obtained. The simulated circuit are in good agreement.

REFERENCES

[1] B. Bryant and M. K. Kazimierczuk, "Voltage-loop power-stage transfer functions with MOSFET delay for boost PWM converter operating in CCM," *IEEE Trans. Ind. Electron.*, vol. 54, no. 1, pp. 347-353, Feb. 2007.  
 [2] X. Wu, J. Zhang, X. Ye, and Z. Qian, "Analysis and derivations for a family ZVS converter based on a new active clamp ZVS cell," *IEEE Trans. Ind. Electron.*, vol. 55, no. 2, pp. 773-781, Feb. 2008.  
 [3] D. C. Lu, K. W. Cheng, and Y. S. Lee, "A single-switch continuous-conduction-mode boost converter with reduced

reverse-recovery and switching losses," *IEEE Trans. Ind. Electron.*, vol. 50, no. 4, pp. 767-776, Aug. 2003.

[4] N. Mohan, T. M. Undeland, and W. P. Robbins, *Power Electronics*, Third Edition, John Wiley & Sons, Inc., 2003.

[5] N. P. Papanikolaou and E. C. Tatakis, "Active voltage clamp in flyback converters operating in CCM mode under wide load variation," *IEEE Trans. Ind. Electron.*, vol. 51, no. 3, pp. 632- 640, Jun. 2004.

[6] B. R. Lin and F. Y. Hsieh, "Soft-switching zeta-flyback converter with a buck-boost type of active clamp," *IEEE Trans. Ind. Electron.*, vol. 54, no. 5, pp. 2813-2822, Oct. 2007.

[7] C. M. Wang, "A novel ZCS-PWM flyback converter with a simple ZCS-PWM commutation cell," *IEEE Trans. Ind. Electron.*, vol. 55, no. 2, pp. 749-757, Feb. 2008.

[8] G. W. Wester and R. D. Middlebrook, "Low-frequency characterization of switched dc-to-dc converters," *IEEE Trans. Aerosp. Electron. Syst.*, vol. AES-9, no. 5, pp. 376-385, May 1973.

[9] R. D. Middlebrook and S. Cuk, "A general unified approach to modelling switching converter power stages," in *Proc. IEEE Power Electron. Spec. Conf.*, 1976, pp. 18-34.

[10] H. Bodur and A. Faruk Bakan, "A new ZCT-ZVT PWM DC-DC converter," *IEEE Trans. Power Electron.*, vol. 19, no. 3, pp. 676-684, May 2004.

[11] G. Hua, C. Lea, and F. C Lee, "Novel zero voltage transition PWM converter," *IEEE Trans. Power Electron.*, vol. 9, no. 2, pp. 55-61, Mar. 1994.

[12] J. A Bassett, "New, zero voltage switching, high frequency boost converter topology for power factor correction," in *Proc. IEEE INTELEC*, The Hague, The Netherlands, 1995, pp. 813-820.

[13] D. M. Xu, C. Yang, L. Ma, C. Qiao, and Z. Qian, "A novel single phase active clamped PFC converter," in *Proc. IEEE APEC*, Atlanta, GA, 1997, pp. 266-271.



**Dr.K.Sri Gowri** received the B.Tech degree from SVU college of Engineering, Tirupati in 1997, the M.Tech degree from RGM College of Engineering and Technology, Nandyal and has been awarded Ph.D in the area of Power Electronic Control of Electric Drives from JNTU Kakinada in 2010. She is currently Professor in the Department of EEE in RGM CET, Nandyal, A.P. Her areas of interest include Power Electronics, Pulse Width Modulation Techniques, Drives and Control, Renewable Sources of Energy. E-mail: gowrivasu.3@gmail.com



**J.Shankaraiah** is born in 1987 in India. He is graduated from JNTUA in 2009. Presently he is doing post graduation in Power Electronics and Electrical drives Specialization at J.N.T.U.A. Anantapur. His main areas of interest include

Induction motor drives, Electrical machines, power Electronic converters and Power Electronic Drives.

Email:sankar3ysrs@gmail.com



**G. Kumaraswamy** is born in 1983 in India. He is graduated from JNTU University in 2005 and pursued Post graduation from the same university. He is currently working as a Assistant professor in the department of electrical and electronics engineering R.G.M

college of engineering and technology, Nandyal, Andhra Pradesh, India. He has eight years of teaching experience. He has attended several National workshops. His main areas of research include Photovoltaic cells, Multilevel inverters. Email:kumar1718@gmail.com